Journal of Mathematical Modeling
Vol. 13, No. 3, 2025, pp. 445-466. Research Article

JMM

A three-layered compartmental model of Nipah virus transmission with analysis

Hossien Gholami[†], Mortaza Gachpazan[†], Majid Erfanian[‡*]

[†]*Department of Applied Mathematics, Faculty of Mathematical Science, Ferdowsi University of Mashhad, Mashhad, Iran*
[‡]*Department of Science, School of Mathematical Sciences, University of Zabol, Zabol, Iran*
Email(s): gholamihossein500@gmail.com, gachpazan@um.ac.ir, erfaniyan@uoz.ac.ir

Abstract. In this work, we have proposed a three-layered (fruit bat-to-fruit-to-human) compartmental model for the description of the spread of the Nipah virus. We have proved the positivity and boundedness of the model's solutions. The bounded nature of the answers also suggests that the disease spread process eventually reaches a steady state, which helps preventing unrealistic predictions. We have shown that a disease-free equilibrium point has local stability. Besides, the global stability of disease-free equilibrium point has been demonstrated with the help of a fluctuation lemma. We have fitted our model with the reported cases of infection and death in Bangladesh. From sensitivity analysis, we understand which parameters are more sensitive to change. Lastly, we have solved the model equations numerically utilizing the Runge-Kutta method to examine the effect of various parameters on the population of the model classes.

Keywords: Three-layered compartmental model, equilibria, stability, sensitivity analysis.
AMS Subject Classification 2010: 92B05, 92D25, 92D30, 37N25, 34D23.

1 Introduction

Zoonotic pathogens have been recognized as a threat to global public health since the end of the last millennium. As a zoonotic disease, the Nipah virus has a high potential to cause a global pandemic. The natural hosts of Nipah virus are fruit bats (especially Pteropus) and the virus is transmitted to humans and other animals through direct or indirect contact with the secretions of these bats [18]. According to the World Health Organization, the mortality rate of this disease is estimated to be $40-75\%$. Due to climate change and changes in natural habitats, the risk of the global spread of the Nipah virus has increased. The lack of studies and data in the field of mathematical modeling presents a valuable opportunity for

*Corresponding author
Received: 13 November 2024 / Revised: 24 December 2024 / Accepted: 16 January 2025
DOI: 10.22124/jmm.2025.28949.2577

researchers to help understand and control this disease by using new methods and updated data. Mathematical modeling is one of the powerful tools that can be used to study and understand Nipah disease and its growth and spread factors. Mathematical modeling is usually developed by using mathematical equations to describe the interactions between different and influential factors of the Nipah virus, which are generally considered part of a dynamic system. Loyinmi et al. [14], for instance, introduced a bat-to-pig-to-human route for Nipah virus transmission. They incorporated four control parameters, personal prevention, effort of treatment on the infected human class, biosecurity and public health intervention, and effort of treatment on the pig population. Shah et al. [19] examined a two-layered compartmental model comprised of a bat and a human. Their model advocated controls as preventive measures in terms of burying infected bats and dead bodies of humans, spraying insecticides on infected bats, and in time hospitalization for infected humans. Goswami and Hategekimana [11] enlarged a compartmental model of Nipah virus transmission. They extended the model to the optimal control problem and analyzed it by utilizing Pontryagins Maximum Principle. Samreen et al. [18] presented a compartmental model comprised of seven classes with Caputo fractional derivative, considering the effects of unsuitable contact with an infectious corpse as a potential pathway for Nipah virus transmission. Li et al. [13] formulated a compartmental model using the Caputo fractional and fractal-fractional operators to study the dynamics of Nipah virus infection. Barua et al. [5] suggested a three-layered model for the NiV transmission. They took into consideration seasonal effects such as varying transmission rates from bats and the birth rate of bats. Das et al. [8] examined a coupled pig-human to realize the dynamics of NiV transmission. To display the scenario, two parameters representing biosecurity level and selective culling rate are incorporated into their system. While research on the Nipah virus is limited compared to other infectious diseases, several studies have explored the dynamics of disease spread in similar pathogens, often using optimal control models ([4, 8, 11, 14, 18, 19]). However, these studies typically focus on general epidemiological patterns and do not specifically address the role of infected fruit as a key vector, which is a significant feature of Nipah virus transmission. Our work builds upon these existing models by incorporating the unique transmission dynamics associated with fruit-borne infection, providing a more nuanced approach to understanding disease spread. In addition, interested readers can see the mathematical modeling of other infectious diseases such as HIV/AIDS, Asthma and COVID-19 in [1–3, 12, 15–17, 21–24] and the references therein.

This work is organized as follows. The structure and formulation of the model are presented in section 2. Additionally, some basic properties of the model are proven in this section. The computation of the basic reproduction number and the types of endemic equilibrium points are provided in sections 3 and sections 4, respectively. Stability analysis of the equilibrium points is presented in section 5. Numerical simulations including parameter estimation and sensitivity analysis are carried out in section 6. Finally, the conclusion is presented in section 7.

2 Mathematical model formulation

Our objective is to model disease transmission across three different species. Specifically, we propose a compartmental framework that accounts for transmission between fruit bats and fruit bats, fruit bats and fruits, fruits and fruits, fruits and humans, as well as human-to-human transmission. However, we do not consider transmission from humans to either of the fruits or fruit bats or from fruit bats to humans, as these transmission routes are assumed to have negligible probabilities (see Figure 1). In this

study, the human population is categorized into susceptible, infected, and recovered groups, whereas the populations of the fruit and fruit bat species are each divided into two categories: susceptible and infected. We have not considered a recovered group for these two species. The mathematical model will be constituted by dividing the populations into seven compartments. 1. The susceptible fruit bats S_B, 2. infected fruit bats I_B, 3. susceptible fruits S_F, 4. infected fruits I_F, 5. susceptible humans S_H, 6. infected humans I_H, and 7. recovered humans R_H. The total population of fruit bats at time t is denoted by $N_B(t) = S_B(t) + I_B(t)$. Then, the total population of fruits at time t is represented by $N_F(t) = S_F(t) + I_F(t)$, and the total population of human beings at time t is introduced by $N_H(t) = S_H(t) + I_H(t) + R_H(t)$.

The fruit bat population is recruited at the rate of Ψ_B. They die due to natural causes at the rate of μ_B.

Table 1: Illustration of the model variables and parameters

Variables/Parameters	Illustration
$S_H(t)$	Agent of susceptible humans at time t
$I_H(t)$	Agent of infected humans at time t
$R_H(t)$	Agent of recovered humans at time t
$S_F(t)$	Agent of susceptible fruits at time t
$I_F(t)$	Agent of infected fruits at time t
$S_B(t)$	Agent of susceptible fruit bats at time t
$I_B(t)$	Agent of infected fruit bats at time t
$N_H(t)$	Total size of human population at time t
$N_F(t)$	Total size of fruit population at time t
$N_B(t)$	Total size of fruit bat population at time t
Ψ_H	Rate of recruitment from birth and immigration for humans
Ψ_F, Ψ_B	Rate of recruitment for fruits and fruit bats, respectively
β_1	Rate of transmission from infected (RTI) to susceptible humans
$\beta_2(\beta_3)$	RTI fruits to susceptible humans(fruits)
$\beta_4(\beta_5)$	RTI fruit bats to susceptible fruits (fruit bats)
μ_H	Natural death rate for humans
μ_F	Decay rate for fruits
μ_B	Natural death rate for fruit bats
$\delta_H(\delta_B)$	Death rate due to Nipah virus for humans(fruit bats)
σ_H	Recovery rate of infected humans
γ_H	Rate of reduction of the immunity after the recovery

Furthermore, when susceptible fruit bats acquire the infection, they become infected at the rate of β_5 and transition to the infected compartment. Infected fruit bats die naturally at the rate of μ_B and there is also a death rate due to the Nipah virus, denoted by δ_B. Thus, we have

$$\frac{dS_B(t)}{dt} = \Psi_B - \beta_5 S_B(t) I_B(t) - \mu_B S_B(t), \qquad \frac{dI_B(t)}{dt} = \beta_5 S_B(t) I_B(t) - (\mu_B + \delta_B) I_B(t). \tag{1}$$

The recruitment rate for the population of susceptible fruit is denoted by Ψ_F. Fruits decay at the rate of μ_F. Susceptible fruits become infected through contact with infected fruits or infected fruit bats at the rates of β_3 and β_4, respectively. Infected fruits also decay at the rate of μ_F. The following differential

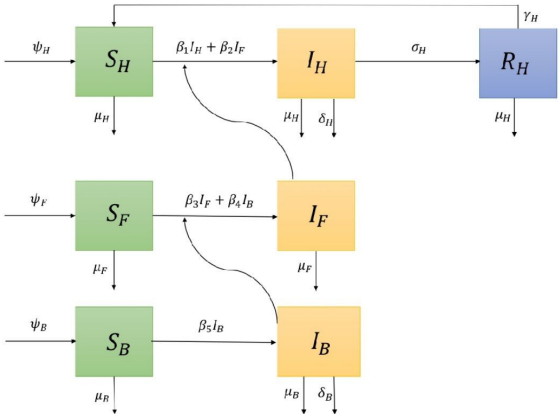

Figure 1: Interaction diagram of human, fruit, and fruit bat populations for the Nipah virus transmission

equations describe the dynamics of the fruit population

$$\begin{aligned}\frac{dS_F(t)}{dt} &= \Psi_F - \beta_3 S_F(t) I_F(t) - \beta_4 S_F(t) I_B(t) - \mu_F S_F(t),\\ \frac{dI_F(t)}{dt} &= \beta_3 S_F(t) I_F(t) + \beta_4 S_F(t) I_B(t) - \mu_F I_F(t).\end{aligned} \tag{2}$$

and

$$\begin{aligned}\frac{dS_H(t)}{dt} &= \Psi_H - \beta_1 S_H(t) I_H(t) - \beta_2 S_H(t) I_F(t) - \mu_H S_H(t) + \gamma_H R_H(t),\\ \frac{dI_H(t)}{dt} &= \beta_1 S_H(t) I_H(t) + \beta_2 S_H(t) I_F(t) - (\mu_H + \delta_H + \sigma_H) I_H(t),\\ \frac{dR_H(t)}{dt} &= \sigma_H I_H(t) - (\mu_H + \gamma_H) R_H(t).\end{aligned} \tag{3}$$

Compounding (1) to (3), we have the following system of equations

$$\begin{aligned}\frac{dS_H(t)}{dt} &= \Psi_H - \beta_1 S_H(t) I_H(t) - \beta_2 S_H(t) I_F(t) - \mu_H S_H(t) + \gamma_H R_H(t),\\ \frac{dI_H(t)}{dt} &= \beta_1 S_H(t) I_H(t) + \beta_2 S_H(t) I_F(t) - (\mu_H + \delta_H + \sigma_H) I_H(t),\\ \frac{dR_H(t)}{dt} &= \sigma_H I_H(t) - (\mu_H + \gamma_H) R_H(t),\\ \frac{dS_F(t)}{dt} &= \Psi_F - \beta_3 S_F(t) I_F(t) - \beta_4 S_F(t) I_B(t) - \mu_F S_F(t),\\ \frac{dI_F(t)}{dt} &= \beta_3 S_F(t) I_F(t) + \beta_4 S_F(t) I_B(t) - \mu_F I_F(t),\\ \frac{dS_B(t)}{dt} &= \Psi_B - \beta_5 S_B(t) I_B(t) - \mu_B S_B(t),\\ \frac{dI_B(t)}{dt} &= \beta_5 S_B(t) I_B(t) - (\mu_B + \delta_B) I_B(t).\end{aligned} \tag{4}$$

The corresponding initial conditions are

$$\begin{aligned} S_H(t_0) = S_{H0} \geq 0, \quad & I_H(t_0) = I_{H0} \geq 0, \\ R_H(t_0) = R_{H0} \geq 0, \quad & I_B(t_0) = I_{B0} \geq 0 \\ S_F(t_0) = S_{F0} \geq 0, \quad & I_F(t_0) = I_{F0} \geq 0, \\ & S_B(t_0) = S_{B0} \geq 0. \end{aligned}$$

The schematic flow diagram for the Nipah virus transmission is depicted in Figure 1, and in Table 1 the variables and parameters of the model (4) are illustrated. In addition, to prove the positivity and boundedness of solutions of the model (4) we used the theorems mentioned above.

Theorem 1. *With the non-negative initial conditions, the solution set*

$$\{S_H(t), I_H(t), R_H(t), S_F(t), I_F(t), S_B(t), I_B(t)\}$$

will be non-negative for all $t \geq 0$.

Proof. We use the proof by contradiction to show that the state variable S_H of the model is positive for all $t \geq 0$. Assume that a trajectory crosses the positive cone at time t_1 such that

$$S_H(t_1) = 0, \quad \frac{dS_H(t_1)}{dt} \leq 0, \quad I_H(t) > 0, \quad R_H(t) > 0, \quad S_F(t) > 0,$$

$$I_F(t) > 0, \quad S_B(t) > 0, \quad I_B(t) > 0 \quad \text{for all } t \in (0, t_1).$$

Utilizing the first equation of model (4), the first supposition results in

$$\frac{dS_H(t_1)}{dt} = \Psi_H + \gamma_H R_H(t_1) > 0,$$

which contradicts the first supposition that $\frac{dS_H(t_1)}{dt} < 0$. Therefore, $S_H(t)$ remains positive for all $t \geq 0$. Now, we extend this argument to consider the case where $\gamma_H R_H$ is very small or negligible. Suppose at some time t_1, $\gamma_H R_H \approx 0$. In this case, the equation for the change in $S_H(t)$ becomes

$$\frac{dS_H}{dt} = \Psi_H - \beta_1 S_H(t) I_H(t) - \beta_2 S_H(t) I_F(t) - \mu_H S_H(t).$$

Here, β_1, β_2 and μ_H are three main factors could negatively impact $S_H(t)$. However, since Ψ_H (the recruitment rate) is always positive, we can conclude that the changes in $S_H(t)$ are counteracted by this positive term. To prove that $S_H(t)$ remains positive under these conditions, assume that $S_H(t) = 0$ at some time t_0. At this point, the equation for $\frac{dS_H}{dt}$ simplifies to

$$\frac{dS_H}{dt} = \Psi_H.$$

Since $\Psi_H > 0$, we see that even if $S_H(t) = 0$ at t_0, $S_H(t)$ will start increasing again due to the recruitment of new individuals at rate Ψ_H, which compensates for the negative effects from transmission and mortality. Using the second equation of model (4),

$$\frac{dI_H(t)}{dt} = \lambda S_H(t) - (\mu_H + \delta_H + \sigma_H) I_H(t),$$

where $\lambda = \beta_1 I_H(t) + \beta_2 I_F(t)$. Since $S_H(t)$ is non-negative for all $t \geq 0$, we obtain

$$\frac{dI_H}{dt} \geq -(\mu_H + \delta_H + \sigma_H) I_H(t),$$

Which, when solved, yields $I_H(t) \geq I_{H0} \exp(-(\mu_H + \delta_H + \sigma_H)t)$. Thus, $I_H(t) \geq 0$ for all $t \geq 0$. Next, from the third equation of model (4), we have

$$\frac{dR_H}{dt} = \sigma_H I_H(t) - (\mu_H + \gamma_H) R_H(t) \geq -(\mu_H + \gamma_H) R_H(t),$$

Solving this gives $R_H(t) \geq R_{H0} \exp(-(\mu_H + \gamma_H)t) \geq 0$. By similar reasoning, we can conclude that $S_F(t) \geq 0$, $I_F(t) \geq 0$, $S_B(t) \geq 0$, and $I_B(t) \geq 0$ for all $t \geq 0$. Thus, any solution of the model (4) is non-negative for all $t \geq 0$. □

Theorem 2. *The region below is bounded.*

$$\Omega = \left\{ (S_H, I_H, R_H, S_F, I_F, S_B, I_B) \in \mathbb{R}^3_+ \times \mathbb{R}^2_+ \times \mathbb{R}^2_+ : 0 < N_H \leq \frac{\Psi_H}{\mu_H}, 0 < N_F \leq \frac{\Psi_F}{\mu_F}, 0 < N_B \leq \frac{\Psi_B}{\mu_B} \right\},$$

Proof. For $N_H(t)$ we have

$$\frac{dN_H(t)}{dt} = \frac{dS_H(t)}{dt} + \frac{dI_H(t)}{dt} + \frac{dR_H(t)}{dt} = \Psi_H - \mu_H N_H(t) - \delta_H I_H(t).$$

Obviously,

$$\frac{dN_H(t)}{dt} \leq \Psi_H - \mu_H N_H(t).$$

It yields that, $N_H(t) \leq \frac{\Psi_H}{\mu_H} + (N_{H0} - \frac{\Psi_H}{\mu_H}) e^{-\mu_H t}$. Considering $t \to \infty$, we have,

$$\lim_{t \to \infty} sup N_H(t) \leq \frac{\Psi_H}{\mu_H}.$$

With a similar argumentation, we can show that $N_F(t) \leq \frac{\Psi_F}{\mu_F}$ and $N_B(t) \leq \frac{\Psi_B}{\mu_B}$. Therefore, the model is bounded. □

3 Computation of the basic reproduction number $\mathscr{R}_0$

The basic reproduction number of the model (4) is denoted by $\mathscr{R}_0$. How extensively the disease spreads depends on the value of the basic reproduction number $\mathscr{R}_0$. Before calculating $\mathscr{R}_0$, it is necessary to find the disease-free equilibrium point of the model (4) by setting the right-hand sides (R.H.S) of the equations to zero and then substituting $I_H = 0$, $R_H = 0$, $I_F = 0$, and $I_B = 0$. Hence, we get

$$E^0 = (S_H^0, 0, 0, S_F^0, 0, S_B^0, 0) = (\frac{\Psi_H}{\mu_H}, 0, 0, \frac{\Psi_F}{\mu_F}, 0, \frac{\Psi_B}{\mu_B}, 0).$$

To compute the basic reproduction number $\mathscr{R}_0$ for the model (4), we apply the next-generation matrix method which is established in [9].

Theorem 3. *For the model (4) the basic reproduction number is* $\mathscr{R}_0 = \max\{\mathscr{R}_0^H, \mathscr{R}_0^F, \mathscr{R}_0^B\}$ *where* $\mathscr{R}_0^H = \frac{\beta_1\Psi_H}{\mu_H(\mu_H+\delta_H+\sigma_H)}$, $\mathscr{R}_0^F = \frac{\beta_3\Psi_F}{\mu_F^2}$, *and* $\mathscr{R}_0^B = \frac{\beta_5\Psi_B}{\mu_B(\mu_B+\delta_B)}$.

Proof. We decompose the right-hand sides of the equations that directly lead to the spread of the Nipah virus. Therefore, the second, fifth, and seventh equations of the model (4) correspond to the infected compartments. Thus, we rewrite the mentioned equations as $\mathscr{F} - \mathscr{V}$, where

$$\mathscr{F} = \begin{bmatrix} \beta_1 S_H(t) I_H(t) + \beta_2 S_H(t) I_F(t) \\ \beta_3 S_F(t) I_F(t) + \beta_4 S_F(t) I_B(t) \\ \beta_5 S_B(t) I_B(t) \end{bmatrix}, \qquad \mathscr{V} = \begin{bmatrix} (\mu_H + \delta_H + \sigma_H) I_H(t) \\ \mu_F I_F(t) \\ (\mu_B + \delta_B) I_B(t) \end{bmatrix}.$$

We evaluate the derivative of $\mathscr{F}$ and $\mathscr{V}$ at disease-free equilibrium point (E^0) and we get two matrices F and V, where

$$F = \frac{\partial \mathscr{F}(E^0)}{\partial x_j} = \begin{bmatrix} \frac{\beta_1\Psi_H}{\mu_H} & \frac{\beta_2\Psi_H}{\mu_H} & 0 \\ 0 & \frac{\beta_3\Psi_F}{\mu_F} & \frac{\beta_4\Psi_F}{\mu_F} \\ 0 & 0 & \frac{\beta_5\Psi_B}{\mu_B} \end{bmatrix}, \quad V = \frac{\partial \mathscr{V}(E^0)}{\partial x_j} = \begin{bmatrix} \mu_H + \delta_H + \sigma_H & 0 & 0 \\ 0 & \mu_F & 0 \\ 0 & 0 & \mu_B + \delta_B \end{bmatrix}.$$

where $x_j = I_H, I_F$, and I_B. The next-generation matrix is defined as

$$FV^{-1} = \left[\frac{\partial \mathscr{F}(E^0)}{\partial x_j}\right]\left[\frac{\partial \mathscr{V}(E^0)}{\partial x_j}\right]^{-1} = \begin{bmatrix} \frac{\beta_1\Psi_H}{\mu_H(\mu_H+\delta_H+\sigma_H)} & \frac{\beta_2\Psi_H}{\mu_H\mu_F} & 0 \\ 0 & \frac{\beta_3\Psi_F}{\mu_F^2} & \frac{\beta_4\Psi_F}{\mu_F(\mu_B+\delta_B)} \\ 0 & 0 & \frac{\beta_5\Psi_B}{\mu_B(\mu_B+\delta_B)} \end{bmatrix}.$$

Eigenvalues of the FV^{-1} matrix are as follows

$$\frac{\beta_1\Psi_H}{\mu_H(\mu_H+\delta_H+\sigma_H)}, \qquad \frac{\beta_3\Psi_F}{\mu_F^2}, \qquad \frac{\beta_5\Psi_B}{\mu_B(\mu_B+\delta_B)}.$$

$\mathscr{R}_0$ is defined as the spectral radius of the FV^{-1} matrix. So,

$$\mathscr{R}_0 = \max\left\{\frac{\beta_1\Psi_H}{\mu_H(\mu_H+\delta_H+\sigma_H)}, \frac{\beta_3\Psi_F}{\mu_F^2}, \frac{\beta_5\Psi_B}{\mu_B(\mu_B+\delta_B)}\right\}.$$

□

4 Types of endemic equilibrium points of the model

In this section, depending on whether the Nipah virus disease is endemic only among the human population, both the human and fruit populations, or all three populations (human, fruit, and fruit bats) it is possible to imagine various equilibrium points for the model of (4). First, the human and fruit endemic equilibrium, as well as the human-only endemic equilibrium, are defined as $E^\star := (S_H^\star, I_H^\star, R_H^\star, S_F^\star, I_F^\star, S_B^\star, 0)$, and $\tilde{E} := (\tilde{S}_H, \tilde{I}_H, \tilde{R}_H, \tilde{S}_F, 0, \tilde{S}_B, 0)$.

Lemma 1. *If the disease is only endemic in population of human, then the equilibrium* $\tilde{E} := (\tilde{S}_H, \tilde{I}_H, \tilde{R}_H, \tilde{S}_F, 0, \tilde{S}_B, 0)$ *exists if* $\mathscr{R}_0^H > 1$.

Proof. According to the assumptions of Lemma, we have the following system

$$\frac{dS_H}{dt} = \Psi_H - \beta_1 S_H I_H - \mu_H S_H + \gamma_H R_H, \quad \frac{dI_H}{dt} = \beta_1 S_H I_H - (\mu_H + \delta_H + \sigma_H) I_H,$$
$$\frac{dR_H}{dt} = \sigma_H I_H - (\mu_H + \gamma_H) R_H, \quad \frac{dS_F}{dt} = \Psi_F - \mu_F S_F, \quad \frac{dS_B}{dt} = \Psi_B - \mu_B S_B.$$

We assume the right-hand sides of all five equations above is equal to zero. By solving the reduced system above, we obtain

$$\tilde{S}_H = \frac{\mu_H + \delta_H + \sigma_H}{\beta_1}, \tilde{I}_H = \frac{\mu_H(\mu_H + \gamma_H)(\mu_H + \delta_H + \sigma_H)(\mathscr{R}_0^H - 1)}{\beta_1(\mu_H^2 + \mu_H\delta_H + \mu_H\sigma_H + \mu_H\gamma_H + \gamma_H\delta_H)},$$
$$\tilde{R}_H = \frac{\mu_H\sigma_H(\mu_H + \delta_H + \sigma_H)(\mathscr{R}_0^H - 1)}{\beta_1(\mu_H^2 + \mu_H\delta_H + \mu_H\sigma_H + \mu_H\gamma_H + \gamma_H\delta_H)}, \tilde{S}_F = \frac{\Psi_F}{\mu_F}, \tilde{S}_B = \frac{\Psi_B}{\mu_B}.$$

So, $\mathscr{R}_0^H > 1$, exists, if and only if $\tilde{E}$. □

Lemma 2. *The* $E^\star := (S_H^\star, I_H^\star, R_H^\star, S_F^\star, I_F^\star, S_B^\star, 0)$ *exists if* $\mathscr{R}_0^F > 1$.

Proof. According to the assumptions of the lemma, the following system can be considered

$$\begin{aligned}
\frac{dS_H}{dt} &= \Psi_H - \beta_1 S_H I_H - \beta_2 S_H I_F - \mu_H S_H + \gamma_H R_H,\\
\frac{dI_H}{dt} &= \beta_1 S_H I_H + \beta_2 S_H I_F - (\mu_H + \delta_H + \sigma_H) I_H,\\
\frac{dR_H}{dt} &= \sigma_H I_H - (\mu_H + \gamma_H) R_H, \qquad \frac{dS_F}{dt} = \Psi_F - \beta_3 S_F I_F - \mu_F S_F,\\
\frac{dI_F}{dt} &= \beta_3 S_F I_F - \mu_F I_F, \qquad \frac{dS_B}{dt} = \Psi_B - \mu_B S_B.
\end{aligned} \tag{5}$$

We assume the right-hand sides of all six equations above is zero. Also by solving Eq. (5) we have $S_B^\star = \Psi_B/\mu_B$. After that, we solve equations related to fruits and obtain

$$S_F^\star = \frac{\mu_F}{\beta_3}, \qquad I_F^\star = \frac{\beta_3\Psi_F - \mu_F^2}{\beta_3\mu_F} = \frac{\mu_F(\mathscr{R}_0^F - 1)}{\beta_3}.$$

It shows that $I_F^\star$ exists if and only if $\mathscr{R}_0^F > 1$. Replacing $I_F^\star$ into the place of $I_F(t)$ in equations related to humans, we get

$$\begin{aligned}
\frac{dS_H}{dt} &= \Psi_H - \beta_1 S_H I_H - \beta_2 S_H I_F^\star - \mu_H S_H + \gamma_H R_H,\\
\frac{dI_H}{dt} &= \beta_1 S_H I_H + \beta_2 S_H I_F^\star - (\mu_H + \delta_H + \sigma_H) I_H,\\
\frac{dR_H}{dt} &= \sigma_H I_H - (\mu_H + \gamma_H) R_H.
\end{aligned}$$

To obtain the $S_H^\star$, $I_H^\star$ and $R_H^\star$, we require to solve the following system of equations

$$\begin{aligned}
\Psi_H - \beta_1 S_H I_H - \beta_2 S_H I_F^\star - \mu_H S_H + \gamma_H R_H &= 0,\\
\beta_1 S_H I_H + \beta_2 S_H I_F^\star - (\mu_H + \delta_H + \sigma_H) I_H &= 0,\\
\sigma_H I_H - (\mu_H + \gamma_H) R_H &= 0.
\end{aligned} \tag{6}$$

We obtain R_H and I_H of the above system and substitute it into the first equation of (6), then we have

$$S_H = \frac{\Psi_H(\mu_H+\gamma_H)+\gamma_H\sigma_H I_H}{(\beta_1 I_H+\beta_2 I_F^\star+\mu_H)(\mu_H+\gamma_H)}. \tag{7}$$

Replacing (7) into the second equation of (6), then we get a quadratic equation in terms of I_H as follows

$$\beta_1[(\mu_H+\delta_H)(\mu_H+\gamma_H)+\mu_H\sigma_H]I_H^2-\beta_2\Psi_H(\mu_H+\gamma_H)I_F^\star+$$

$$[\beta_2 I_F^\star(\mu_H+\gamma_H)(\mu_H+\delta_H)+\mu_H\sigma_H+\mu_H(\mu_H+\gamma_H)(\mu_H+\delta_H+\sigma_H)(1-\mathscr{R}_0^H)]I_H=0$$

Therefore, the $E^\star$ exists. □

Lemma 3. *If for all three species, the disease is endemic among the population then, the endemic equilibrium point* $\hat{E}:=(\hat{S}_H,\hat{I}_H,\hat{R}_H,\hat{S}_F,\hat{I}_F,\hat{S}_B,\hat{I}_B)$ *exist if and only if* $\mathscr{R}_0^B>1$ *and* $\mathscr{R}_0^F>1$.

Proof. We set the right-hand sides of all the equations to zero.

$$\begin{aligned}
\Psi_H-\beta_1 S_H(t)I_H(t)-\beta_2 S_H(t)I_F(t)-\mu_H S_H(t)+\gamma_H R_H(t)&=0,\\
\beta_1 S_H(t)I_H(t)+\beta_2 S_H(t)I_F(t)-(\mu_H+\delta_H+\sigma_H)I_H(t)&=0,\\
\sigma_H I_H(t)-(\mu_H+\gamma_H)R_H(t)&=0,\\
\Psi_F-\beta_3 S_F(t)I_F(t)-\beta_4 S_F(t)I_B(t)-\mu_F S_F(t)&=0,\\
\beta_3 S_F(t)I_F(t)+\beta_4 S_F(t)I_B(t)-\mu_F I_F(t)&=0,\\
\Psi_B-\beta_5 S_B(t)I_B(t)-\mu_B S_B(t)&=0,\\
\beta_5 S_B(t)I_B(t)-(\mu_B+\delta_B)I_B(t)&=0.
\end{aligned} \tag{8}$$

From solving the equations for fruit bats (the last two equations of (8)), we have

$$\hat{S}_B=\frac{\mu_B+\delta_B}{\beta_5},\quad \hat{I}_B=\frac{\Psi_B}{\mu_B+\delta_B}-\frac{\mu_B}{\beta_5}.$$

Replacing the value of $\hat{I}_B$ into the equations for fruits (the fourth and fifth equations of (8)), we get

$$\begin{aligned}
\Psi_F-\beta_3 S_F(t)I_F(t)-\beta_4 S_F(t)\hat{I}_B(t)-\mu_F S_F(t)&=0,\\
\beta_3 S_F(t)I_F(t)+\beta_4 S_F(t)\hat{I}_B(t)-\mu_F I_F(t)&=0.
\end{aligned}$$

By solving the above equations we obtain $\hat{I}_F$ and replacing the value of $\hat{I}_F$ into the first three equations of (8), we obtain $\hat{I}_H$. Similarly, as in the proof of the previous lemma, we can observe that the endemic equilibrium exists if $\mathscr{R}_0^B>1$ and $R_0^F>1$. □

5 Stability analysis

In this section, we discuss about stability of equilibrium points.

Theorem 4. *The* E^0 *is locally asymptotically stable if* $\mathscr{R}_0<1$.

Proof. The Jacobian matrix of (4) at the disease-free equilibrium point (E^0) is given by

$$J(E^0)=\begin{bmatrix} -\mu_H & -\frac{\beta_1\Psi_H}{\mu_H} & \gamma_H & 0 & -\frac{\beta_2\Psi_H}{\mu_H} & 0 & 0 \\ 0 & \frac{\beta_1\Psi_H}{\mu_H}-(\mu_H+\delta_H+\sigma_H) & 0 & 0 & \frac{\beta_2\Psi_H}{\mu_H} & 0 & 0 \\ 0 & \sigma_H & -(\mu_H+\gamma_H) & 0 & 0 & 0 & 0 \\ 0 & 0 & 0 & -\mu_F & -\frac{\beta_3\Psi_F}{\mu_F} & 0 & -\frac{\beta_4\Psi_F}{\mu_F} \\ 0 & 0 & 0 & 0 & \frac{\beta_3\Psi_F}{\mu_F}-\mu_F & 0 & \frac{\beta_4\Psi_F}{\mu_F} \\ 0 & 0 & 0 & 0 & 0 & -\mu_B & -\frac{\beta_5\Psi_B}{\mu_B} \\ 0 & 0 & 0 & 0 & 0 & 0 & \frac{\beta_5\Psi_B}{\mu_B}-(\mu_B+\delta_B) \end{bmatrix},$$

The eigenvalues of $J(E^0)$ are $-\mu_H$, $-(\mu_H+\gamma_H)$, $-\mu_F$, $-\mu_B$, $\frac{\beta_1\Psi_H}{\mu_H}-(\mu_H+\delta_H+\sigma_H)$, $\frac{\beta_3\Psi_F}{\mu_F}-\mu_F$, and $\frac{\beta_5\Psi_B}{\mu_B}-(\mu_B+\delta_B)$. The first four eigenvalues are negative. Thus, E^0 is locally asymptotically stable if

$$\frac{\beta_1\Psi_H}{\mu_H}-(\mu_H+\delta_H+\sigma_H)=(\mu_H+\delta_H+\sigma_H)(\mathscr{R}_0^H-1)<0,$$
$$\frac{\beta_3\Psi_F}{\mu_F}-\mu_F=\mu_F(\mathscr{R}_0^F-1)<0,$$
$$\frac{\beta_5\Psi_B}{\mu_B}-(\mu_B+\delta_B)=(\mu_B+\delta_B)(\mathscr{R}_0^B-1)<0.$$

Thus, it is necessary to $\mathscr{R}_0^H<1$, $\mathscr{R}_0^F<1$, and $\mathscr{R}_0^B<1$. As a consequence, $\mathscr{R}_0<1$. If any one of these inequalities is altered then E^0 is unstable. □

5.1 Global stability of the equilibria

In this subsection, we prove in the form of theorems under what conditions each equilibrium point has global asymptotic stability. To prove that E^0 has global asymptotic stability, we use the fluctuation lemma (see [20]). For a bounded and differentiable function f on $\mathbb{R}_+$, we introduce the notations

$$f^\infty=\limsup_{t\to\infty} f(t),\ \text{and}\ f_\infty=\liminf_{t\to\infty} f(t).$$

Theorem 5. *The disease-free equilibrium point E^0 is globally asymptotically stable if $\mathscr{R}_0<1$.*

Proof. Let $(S_B(t),I_B(t))$ be a solution for (1). By using the fluctuation lemma, there exist a sequence $\{t_n\}$ such that $t_n\to\infty$. We have $I_B(t_n)\to I^\infty$ and $\frac{dI_B}{dt}(t_n)\to\infty$ as $n\to\infty$. From the equation for infected fruit bats, we have

$$\frac{dI_B}{dt}=\beta_5 S_B(t_n)I_B(t_n)-(\mu_B+\delta_B)I_B(t_n),$$

From theorem 2 we have $0\le\frac{\beta_5\Psi_B}{\mu_B}I_B^\infty-(\mu_B+\delta_B)I_B^\infty$. Hence, $0\le(\mu_B+\delta_B)(\mathscr{R}_0^B-1)I_B^\infty$. Since, $\mathscr{R}_0^B<1$, we have $I_B^\infty=0$. By re-using the fluctuation lemma, there exist a sequence $u_n\to\infty$ such that $S_B(u_n)\to S_\infty$ and $\frac{dS_B}{dt}(u_n)\to 0$ as $n\to\infty$. From the equation for susceptible fruit bats we have

$$\frac{dS_B}{dt}(u_n)=\Psi_B-\beta_5 S_B(u_n)I_B(u_n)-\mu_B S_B(u_n).$$

Since, $I_B^\infty = 0$ and assuming $n \to \infty$ we get $(S_B)_\infty = \frac{\Psi_B}{\mu_B} > S_B^\infty$. It follows that $\lim_{t\to\infty} S_B(t) = \frac{\Psi_B}{\mu_B}$. So for subsystem (1) we have

$$\lim_{t\to\infty}(S_B(t), I_B(t)) = (\frac{\Psi_B}{\mu_B}, 0).$$

Applying these results in subsystem (1) for fruits we can prove $\lim_{t\to\infty}(S_F(t), I_F(t)) = (\Psi_F/\mu_F, 0)$ if $\mathscr{R}_0^F < 1$. Ultimately, repeating this procedure for the subsystem (3), it can be seen $\lim_{t\to\infty}(S(t), I(t), R(t)) = (\Psi/\mu, 0, 0)$ if $\mathscr{R}_0^H < 1$. Therefore, E^0 is globally asymptotically stable if $\mathscr{R}_0 < 1$. □

Theorem 6. *The $\tilde{E}$ is globally asymptotically stable if $\mathscr{R}_0^H > 1$, $\mathscr{R}_0^F < 1$ and $\mathscr{R}_0^B < 1$.*

Proof. From $\mathscr{R}_0^F < 1$ and $\mathscr{R}_0^B < 1$, we can understand that there is no transmission from fruit bat to fruit bat, fruit bat to fruit, fruit to fruit, and fruit to human. Thus, the equations for susceptible fruits and susceptible fruit bats will be as follows

$$\frac{dS_F}{dt} = \Psi_F - \mu_F S_F, \quad \frac{dS_B}{dt} = \Psi_B - \mu_B S_B,$$

which obviously, have the globally asymptotically stable equilibria $\frac{\Psi_F}{\mu_F}$ and $\frac{\Psi_B}{\mu_B}$, respectively. Also, the equations for the human subsystem change as follows

$$\begin{aligned}
\frac{dS_H}{dt} &= \Psi_H - \beta_1 S_H I_H - \mu_H S_H + \gamma_H R_H, \\
\frac{dI_H}{dt} &= \beta_1 S_H I_H - (\mu_H + \delta_H + \sigma_H) I_H, \quad \frac{dR_H}{dt} = \sigma_H I_H - (\mu_H + \gamma_H) R_H.
\end{aligned}$$

On the other hand, since $N_H(t) = S_H(t) + I_H(t) + R_H(t)$ thus, $\frac{dN_H}{dt} = \Psi_H - \mu_H N_H - \delta_H I_H$ and we substitute this equation instead of the equation for susceptible humans. So,

$$\begin{aligned}
\frac{dN_H}{dt} &= \Psi_H - \mu_H N_H - \delta_H I_H, \\
\frac{dI_H}{dt} &= \beta_1 I_H (N_H - I_H - R_H) - (\mu_H + \delta_H + \sigma_H) I_H, \quad \frac{dR_H}{dt} = \sigma_H I_H - (\mu_H + \gamma_H) R_H.
\end{aligned}$$

Certainly, $\tilde{N}_H$, $\tilde{I}_H$ and $\tilde{R}_H$ satisfy the equations

$$\begin{aligned}
\Psi_H - \mu_H \tilde{N}_H - \delta_H \tilde{I}_H &= 0, \\
\beta_1 \tilde{I}_H (\tilde{N}_H - \tilde{I}_H - \tilde{R}_H) - (\mu_H + \delta_H + \sigma_H) \tilde{I}_H &= 0, \\
\sigma_H \tilde{I}_H - (\mu_H + \gamma_H) \tilde{R}_H &= 0.
\end{aligned} \tag{9}$$

We consider the Lyapunov function $L(t)$ as

$$L(t) = \frac{\beta_1}{2\delta_H}(N_H - \tilde{N}_H)^2 + (I_H - \tilde{I}_H - \tilde{I}_H \ln(\frac{I_H}{\tilde{I}_H})) + \frac{\beta_1}{2\sigma_H}(R_H - \tilde{R}_H)^2.$$

We show that the time derivative of $L(t)$ along the solution of system (9) is globally negative. Thus,

$$\begin{aligned}
\frac{dL}{dt} &= \frac{\beta_1}{\delta_H}(N_H-\tilde{N}_H)\frac{dN_H}{dt}+(1-\frac{\tilde{I}_H}{I_H})\frac{dI_H}{dt}+\frac{\beta_1}{\sigma_H}(R_H-\tilde{R}_H)\frac{dR_H}{dt}\\
&= \frac{\beta_1}{\delta_H}(N_H-\tilde{N}_H)(\mu_H\tilde{N}_H+\delta_H\tilde{I}_H-\mu_H N_H-\delta_H I_H)\\
&\quad +(1-\frac{\tilde{I}_H}{I_H})(\beta_1 I_H(N_H-I_H-R_H)-\beta_1 I_H(\tilde{N}_H-\tilde{I}_H-\tilde{R}_H))\\
&\quad +\frac{\beta_1}{\sigma_H}(R_H-\tilde{R}_H)(\sigma_H I_H-\sigma_H\tilde{I}_H+(\mu_H+\gamma_H)\tilde{R}_H-(\mu_H+\gamma_H)R_H)\\
&= \frac{\beta_1}{\delta_H}(N_H-\tilde{N}_H)[-\mu_H(N_H-\tilde{N}_H)-\delta_H(I_H-\tilde{I}_H)]\\
&\quad +\beta_1(I_H-\tilde{I}_H)(N_H-\tilde{N}_H-I_H+\tilde{I}_H-R_H+\tilde{R}_H)\\
&\quad +\frac{\beta_1}{\sigma_H}(R_H-\tilde{R}_H)[\sigma_H(I_H-\tilde{I}_H)-(\mu_H+\gamma_H)(R_H-\tilde{R}_H)]\\
&\leq -\beta_1(N_H-\tilde{N}_H)(I_H-\tilde{I}_H)+\beta_1(I_H-\tilde{I}_H)(N_H-\tilde{N}_H)\\
&\quad -\beta_1(I_H-\tilde{I}_H)(R_H-\tilde{R}_H)+\beta_1(R_H-\tilde{R}_H)(I_H-\tilde{I}_H)=0.
\end{aligned}$$

Hence, the endemic equilibrium point $\tilde{E}$ is globally asymptotically stable if $\mathscr{R}_0^H>1$. □

Theorem 7. *The $E^\star:=(S_H^\star,I_H^\star,R_H^\star,S_F^\star,I_F^\star,S_B^\star,0)$ is globally asymptotically stable if $\mathscr{R}_0^F>1$ and $\mathscr{R}_0^B<1$.*

Proof. From $\mathscr{R}_0^B<1$, we can realize that there is no transmission among fruit bats, with the rest of the available modes. By assuming, $N_F(t)=S_F(t)+I_F(t)$ we can substitute an equation instead of susceptible fruits. So

$$\frac{dN_F}{dt}=\Psi_F-\mu_F N_F,\qquad \frac{dI_F}{dt}=\beta_3 I_F(N_F-I_F)-\mu_F I_F. \tag{10}$$

From solving above system results $S_F^\star=\frac{\beta_3}{\mu_F}$ and $I_F^\star=\frac{\Psi_F-\beta_3}{\mu_F}$. Pursuing the scheme of the previous theorem we can show $(S_F^\star,I_F^\star)$ is a globally asymptotically stable fixed point of (10). Now, replacing limiting value $I_F^\star$ of $I_F(t)$ into the human subsystem to obtain

$$\begin{aligned}
&\frac{dS_H}{dt}=\Psi_H-\beta_1 S_H I_H-\beta_2 S_H I_F^\star-\mu_H S_H+\gamma_H R_H,\\
&\frac{dI_H}{dt}=\beta_1 S_H I_H+\beta_2 S_H I_F^\star-(\mu_H+\delta_H+\sigma_H)I_H,\quad \frac{dR_H}{dt}=\sigma_H I_H-(\mu_H+\gamma_H)R_H.
\end{aligned}$$

By assuming, $N_H(t)=S_H(t)+I_H(t)+R_H(t)$, we have the following system for human

$$\begin{aligned}
&\frac{dN_H}{dt}=\Psi_H-\mu_H N_H-\delta_H I_H,\quad \frac{dR_H}{dt}=\sigma_H I_H-(\mu_H+\gamma_H)R_H,\\
&\frac{dI_H}{dt}=(\beta_1 I_H+\beta_2 I_F^\star)(N_H-I_H-R_H)-(\mu_H+\delta_H+\sigma_H)I_H.
\end{aligned}\tag{11}$$

If $V(t)$ is a Lyapunov function so we have

$$V(t)=\frac{1}{2\delta_H}(N_H-N_H^\star)^2+\int_{I_H^\star}^{I_H}\frac{\xi-I_H^\star}{\beta_1\xi+\beta_2 I_F^\star}d\xi+\frac{1}{2\sigma_H}(R_H-R_H^\star)^2.$$

We show that the time derivative of $V(t)$ along the solution of system (11) is globally negative. Thus,

$$\begin{aligned}
\frac{dV}{dt} &= \frac{1}{\delta_H}(N_H - N_H^\star)\frac{dN_H}{dt} + \frac{I_H - I_H^\star}{\beta_1 I_H + \beta_2 I_F^\star}\frac{dI_H}{dt} + \frac{1}{\sigma_H}(R_H - R_H^\star)\frac{dR_H}{dt} \\
&= \frac{1}{\delta_H}(N_H - N_H^\star)(\mu_H N_H^\star + \delta_H I_H^\star - \mu_H N_H - \delta_H I_H) \\
&\quad + (I_H - I_H^\star)\Big[(N_H - N_H^\star) - (I_H - I_H^\star) - (R_H - R_H^\star) \\
&\quad - (\mu_H + \delta_H + \sigma_H)\Big(\frac{I_H}{\beta_1 I_H + \beta_2 I_F^\star} - \frac{I_H^\star}{\beta_1 I_H^\star + \beta_2 I_F^\star}\Big)\Big] \\
&\quad + \frac{1}{\sigma_H}(R_H - R_H^\star)(\sigma_H I_H - \sigma_H I_H^\star + (\mu_H + \gamma_H)R_H^\star - (\mu_H + \gamma_H)R_H) \\
&= \frac{1}{\delta_H}(N_H - N_H^\star)[-\mu_H(N_H - N_H^\star) - \delta_H(I_H - I_H^\star)] \\
&\quad + (I_H - I_H^\star)(N_H - N_H^\star) - (I_H - I_H^\star)^2 - (I_H - I_H^\star)(R_H - R_H^\star) \\
&\quad - (I_H - I_H^\star)(\mu_H + \delta_H + \sigma_H)\Big(\frac{I_H}{\beta_1 I_H + \beta_2 I_F^\star} - \frac{I_H^\star}{\beta_1 I_H^\star + \beta_2 I_F^\star}\Big) \\
&\quad + \frac{1}{\sigma_H}(R_H - R_H^\star)(\sigma_H(I_H - I_H^\star) + (\mu_H + \gamma_H)(R_H - R_H^\star)) \\
&\leq -(N_H - N_H^\star)(I_H - I_H^\star) + (I_H - I_H^\star)(N_H - N_H^\star) \\
&\quad - (I_H - I_H^\star)(R_H - R_H^\star) + (R_H - R_H^\star)(I_H - I_H^\star) \\
&\quad - (I_H - I_H^\star)(\mu_H + \delta_H + \sigma_H)\Big(\frac{I_H}{\beta_1 I_H + \beta_2 I_F^\star} - \frac{I_H^\star}{\beta_1 I_H^\star + \beta_2 I_F^\star}\Big).
\end{aligned}$$

According to assumption (H2) given in [7], the last term of $\frac{dV}{dt}$ is non-positive. So, we conclude $\frac{dV}{dt} \leq 0$. As a result, the $E^\star$ is globally asymptotically stable if $\mathscr{R}_0^F > 1$ and $\mathscr{R}_0^B < 1$. □

Theorem 8. *The endemic equilibrium point* $\hat{E} := (\hat{S}_H, \hat{I}_H, \hat{R}_H, \hat{S}_F, \hat{I}_F, \hat{S}_B, \hat{I}_B)$ *is globally asymptotically stable if* $\mathscr{R}_0^B > 1$.

Proof. In this theorem we assume that the disease is endemic for all cases. The equations of fruit bats can be separated from the equations for fruits and humans. By introducing again $N_B(t) = S_B(t) + I_B(t)$, then we have

$$\frac{dN_B}{dt} = \Psi_B - \mu_B N_B - \delta_B I_B, \quad \frac{dI_B}{dt} = \beta_5(N_B - I_B)I_B - (\mu_B + \delta_B)I_B.$$

Obviously, $\hat{N}_B$ and $\hat{I}_B$ satisfy the equations

$$\Psi_B - \mu_B N_B - \delta_B I_B = 0, \qquad \beta_5(N_B - I_B)I_B - (\mu_B + \delta_B)I_B = 0. \tag{12}$$

From solving system (12) we get $(\hat{S}_B, \hat{I}_B) = (\frac{\mu_B + \delta_B}{\beta_5}, \frac{\mu_B}{\beta_5}(\mathscr{R}_0^B - 1))$. Pursuing the scheme of theorem 6, we can prove $(\hat{S}_B, \hat{I}_B)$ is a globally asymptotically stable fixed point of (12). By replacing $\hat{I}_B$ into the subsystem (2) for fruits, then, we get a similar subsystem in theorem 6. Finally, we deduce that the $\hat{E}$ is globally asymptotically stable if $\mathscr{R}_0^B > 1$. □

Table 2: Values of the model parameters and source

Parameter	Value	Unit	*Source*
Ψ_H	5285	day^{-1}	*Calculated*
Ψ_F	35	day^{-1}	*Fitted*
Ψ_B	0.411	day^{-1}	[4]
β_1	1.39897×10^{-10}	day^{-1}	*Fitted*
β_2	3.49641×10^{-5}	day^{-1}	*Estimated*
β_3	4×10^{-6}	day^{-1}	*Fitted*
β_4	2.53342×10^{-4}	day^{-1}	*Estimated*
β_5	1.55344×10^{-5}	day^{-1}	[10]
μ_H	3.91×10^{-5}	day^{-1}	*Calculated*
μ_F	1.5632×10^{-2}	day^{-1}	*Fitted*
μ_B	1.3699×10^{-4}	day^{-1}	[4]
δ_H	4.36999×10^{-2}	day^{-1}	fact-sheets[1]
δ_B	6.22043×10^{-2}	day^{-1}	*Fitted*
σ_H	2.25626×10^{-2}	day^{-1}	nipah[2]
γ_H	1.53737×10^{-3}	day^{-1}	[4]
$\mathscr{R}_0^H$	0.2852	-	*Calculated*
$\mathscr{R}_0^F$	0.5729	-	*Calculated*
$\mathscr{R}_0^B$	0.7476	-	*Calculated*
$\mathscr{R}_0$	0.7476	-	*Calculated*

6 Numerical simulations

6.1 Estimation of parameters and data fitting

We estimated the parameters in the model (4) utilizing values from outbreaks in Bangladesh to justify some of the theoretical findings. The values of parameters are provided in Table 2. The values of the parameters labeled as fitted or estimated have been obtained through different methods. The fitted parameters were derived through optimization processes and model fitting to experimental data, where the parameter values were adjusted to achieve the best match with the available data. For these parameters, uncertainty is typically assessed through sensitivity analysis. In this study, the sensitivity analysis showed that variations in parameters such as the decay rate for fruits (μ_F) and the death rate due to the Nipah virus for fruit bats (δ_B) could have a significant impact on the model results. On the other hand, the estimated parameters were extracted from reputable scientific sources and previous studies and are typically based on empirical data or estimated values. For these parameters, a more precise evaluation could help improve the accuracy of the results. In the future, the use of new and updated data could help reduce uncertainty.

Finally, the calculated parameters were directly computed from the mathematical relationships and equations of the model. For these types of parameters, it is assumed that the mathematical relationships and model equations are accurate and error-free. The average life expectancy of Bangladesh's human

[1] https://www.who.int/news-room/fact-sheets/detail/nipah-virus
[2] https://www.cdc.gov/vhf/nipah/about/index.html

population in the year 2011 is 70.01[3].

The natural death rate of humans is computed by taking the reciprocal of the average life expectancy (in days), which is

$$\mu_H = \frac{1}{70.01 \times 365} = 0.0000391.$$

We assumed the total human population for the year 2011 is $N_H(0) = 135,180,000$. Then, Ψ_H is estimated using the relation $\Psi_H = \mu_H \times N_H(0)$ and it is computed to be 5285.

Moreover, we considered the Nipah virus yearly reported cases reported in Bangladesh from 2001 to 2015 to validate model results. The data were collected from [6]. However, as with any epidemiological data, it is essential to consider the potential limitations and biases associated with their collection and reporting. While the data used in this study are considered reliable, it is important to acknowledge that there may be limitations in terms of reporting accuracy. For example, underreporting of cases, especially in rural areas, could result in an underestimate of the actual number of cases. Furthermore, reporting practices may vary over time and across regions, potentially leading to inconsistencies in the dataset. Additionally, there are potential biases in the data that should be considered. Moreover, differences in healthcare infrastructure and access to medical services may influence the detection and reporting of cases, which could result in regional biases. These factors should be taken into account when interpreting the data and the results derived from the model. Figure 2 depicts the cumulative disease-induced deaths (shown by red hexagrams) and fitted curve (shown as a purple curve) and displays the cumulative number of infected cases in Bangladesh from 2001 to 2015 (represented by blue diamonds) and fitted curve (shown as a red curve). In both cases, the model fitting showed a good agreement with the collected data. The initial values for the state variables of the proposed model are used as

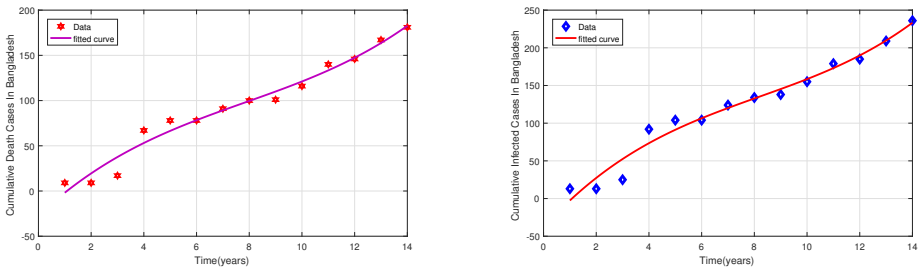

Figure 2: Left: the cumulative disease-induced deaths shown by red hexagrams and fitted curve shown as a purple curve. Right: the cumulative number of infected cases represented by blue diamonds and fitted curve shown as a red curve in Bangladesh from 2001 to 2015.

$$[S_H, I_H, R_H, S_F, I_F, S_B, I_B] = [135179953, 47, 30, 2200, 39, 2930, 70].$$

6.2 Sensitivity Analysis

To find out how much a model is sensitive to changes in parameters, sensitivity analysis is used. The sensitivity index makes it possible to measure the relative changes of the variables compared to the

[3] https://www.macrotrends.net/global-metrics/countries/BGD/bangladesh/life-expectancy

changes of a parameter. For the Y variable that is differentiable for the x parameter, the normalized forward sensitivity index is defined as follows $\Upsilon_x^Y = \frac{x}{Y} \times \frac{\partial Y}{\partial x}$. The basic reproduction number performs a significant role in forecasting disease behavior. Here, because it is not clear which of the three threshold parameters $(\mathscr{R}_0^H, \mathscr{R}_0^F, \mathscr{R}_0^B)$ is the basic reproduction number, hence, we apply the formula above on three threshold parameters concerning the parameters in the model. If the sensitivity index is positive, it shows that the threshold parameter has a direct relationship with the parameter of the model, and if it is negative, it means that the threshold parameter has an inverse relationship with the parameter of the model. According to the Table 3, we can observe that

$$\Upsilon_{\beta_1}^{\mathscr{R}_0^H} = 1, \quad \Upsilon_{\beta_3}^{\mathscr{R}_0^F} = 1, \quad \Upsilon_{\beta_5}^{\mathscr{R}_0^B} = 1.$$

Thus, an increase (or decrease) in these parameters will lead to an increase (decrease) in the same proportion in $\mathscr{R}_0^H$, $\mathscr{R}_0^F$, and $\mathscr{R}_0^B$, respectively. Also, for the rest of the parameters in Table 3, since the sensitivity index is negative, it can be concluded that with the increase (decrease) of these parameters, the value of the corresponding threshold parameter decreases (increases). From Table 3, we can observe that parameters with the largest impact are the decay rate for fruits (μ_F), the natural death rate for fruit bats (μ_B) and the natural death rate for humans (μ_H). The reason why specific parameters such as decay rates are particularly impactful in the sensitivity analysis lies in their direct influence on the transmission dynamics of the disease. In our model, these parameters are crucial because they govern the persistence and availability of susceptible individuals or hosts within the system. The decay rate of fruits is essential in models involving zoonotic diseases like the Nipah virus, where fruit bats are an important vector. If fruit decays faster, it reduces the availability of food resources for bats, which may lead to fewer interactions between bats and humans or other susceptible hosts. As a result, changes in this decay rate can significantly impact disease transmission dynamics, especially in the early stages of an outbreak. The sensitivity index for the parameters β_1 and μ_H is calculated as follows, and for the remaining parameters, it is calculated similarly.

$$\begin{aligned}
\Upsilon_{\beta_1}^{\mathscr{R}_0^H} &= \frac{\beta_1}{\mathscr{R}_0^H} \times \frac{\partial \mathscr{R}_0^H}{\partial \beta_1} = \frac{\Psi_H}{\mu_H(\mu_H+\delta_H+\sigma_H)} \times \frac{\beta_1}{\frac{\beta_1\Psi_H}{\mu_H(\mu_H+\delta_H+\sigma_H)}} = 1, \\
\Upsilon_{\mu_H}^{\mathscr{R}_0^H} &= \frac{\mu_H}{\mathscr{R}_0^H} \times \frac{\partial \mathscr{R}_0^H}{\partial \mu_H} = \frac{\mu_H}{\frac{\beta_1\Psi_H}{\mu_H(\mu_H+\delta_H+\sigma_H)}} \times \frac{-\beta_1\Psi_H(2\mu_H+\delta_H+\sigma_H)}{\mu_H^2(\mu_H+\delta_H+\sigma_H)^2} \\
&= \frac{-(2\mu_H+\delta_H+\sigma_H)}{\mu_H+\delta_H+\sigma_H} = -1.000589729.
\end{aligned}$$

6.3 Impact of different parameters

The Nipah virus has a high potential to cause a global pandemic. Factors such as lack of data and research limitations in its endemic areas such as Malaysia and Bangladesh have caused fewer articles to be published on mathematical modeling of this disease. It needs to be said that all numerical experiments were performed utilizing MATLAB software version of $R2016b$. Here, we have solved the model equations numerically using the Runge-Kutta ($ODE45$) method and the parameter values are presented in Table 2 to portray the impact of different parameters. In Figure 3, the susceptible, infected, and recovered human populations are displayed against the time varies with different choices of recovery rate

Table 3: Sensitivity analysis

Symbols	Sensitivity index of $\mathscr{R}_0^H$	Sensitivity index of $\mathscr{R}_0^F$	Sensitivity index of $\mathscr{R}_0^B$
β_1	1		
μ_H	-1.000589729		
δ_H	-0.659107774		
σ_H	-0.340302496		
β_3		1	
μ_F		-2	
β_5			1
μ_B			-1.180479636
δ_B			-0.997802579

for humans (σ_H). As the recovery rate rises, the population of the recovered population (R_H) rises. The curves of the susceptible class (S_H) converge to zero. Also, the population of the infected class (I_H) reduces. In Figure 4, as the death rate due to the Nipah virus for fruit bats (δ_B) increases, the population of

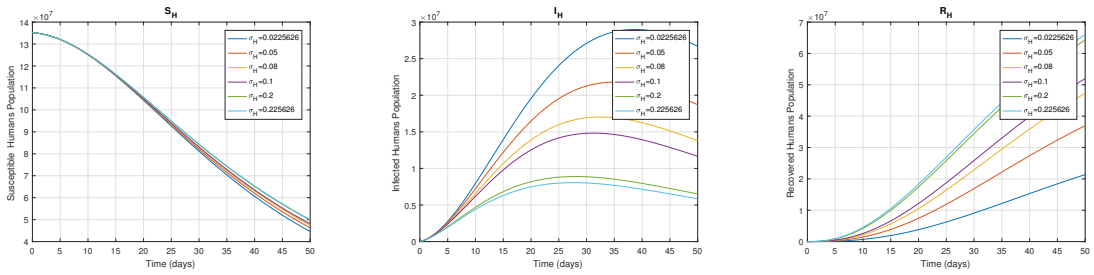

Figure 3: Solution curves depicting the impact of the recovery rate of infected humans (σ_H) on S_H, I_H, and R_H compartments of the model (4) for $\sigma_H = 0.0225626, 0.05, 0.08, 0.1, 0.2$, and 0.225626.

susceptible bats (S_B) decreases less and converges to a certain point. The reason for this is that with the death of infected bats (I_B), their contact with susceptible bats decreases, and also with increasing of this parameter, the population of infected bats reduces significantly and converges to zero. In Figure 5, as the rate of immunity after recovery (γ_H) increases, the population of the recovered class (R_H) decreases more and converges to a certain level. As a consequence, the population of the susceptible class (S_H) increases slowly. Also, the infective curves show the rise in their levels during the initial stage, then decrease.
Figure 6 the left is a three-dimensional surface plot representing $\mathscr{R}_0^B$ as a function of two variables, β_5 (the transmission rate from infected fruit bats to susceptible fruit bats) and μ_B (the natural death rate for fruit bats).

The surface is inclined, indicating that $\mathscr{R}_0^B$ gradually increases with variations in β_5 and μ_B. The surface slope suggests that small changes in these two parameters can significantly impact $\mathscr{R}_0^B$. Steep slopes may indicate a high sensitivity of $\mathscr{R}_0^B$to fluctuations in these parameters.
Figure 6 the right illustrates the three-dimensional sensitivity of $\mathscr{R}_0^B$concerning the variables β_5 and μ_B. A decrease in the natural mortality rate of bats may imply an increase in the bat population, which, in

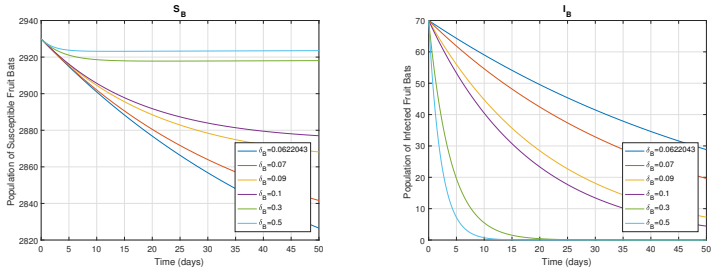

Figure 4: Solution curves depicting the impact of the death rate due to Nipah virus for fruit bats (δ_B) on S_B and I_B compartments of the model (4) for $\delta_B = 0.0622043, 0.07, 0.09, 0.1, 0.3$ and 0.5.

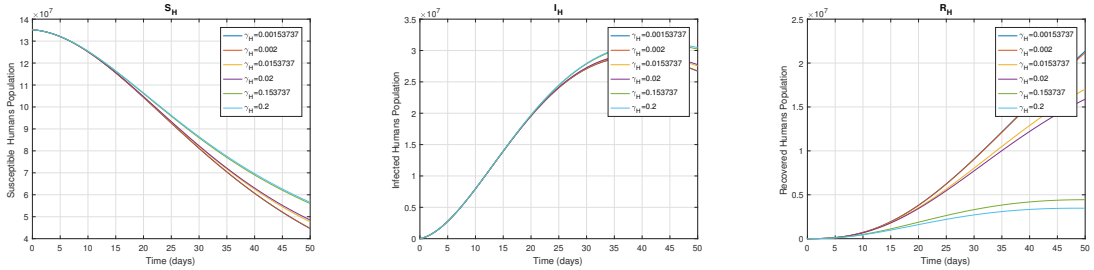

Figure 5: Solution curves depicting the impact of reduction rate of the immunity after the recovery (γ_H) on S_H, I_H, and R_H compartments of the model (4) for $\gamma_H = 0.00153737, 0.02, 0.0153737, 0.02, 0.153737$ and 0.2.

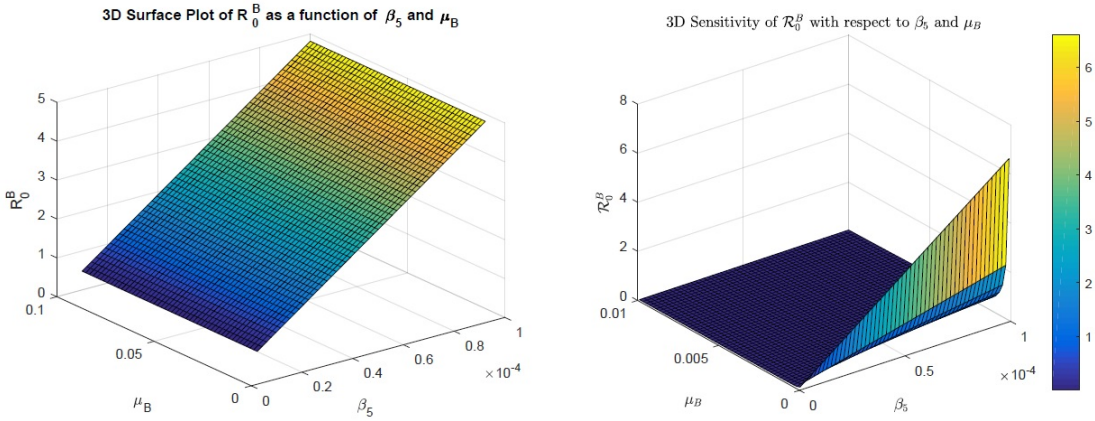

Figure 6: Left: 3D surface plot of $\mathscr{R}_0^B$ as a function of β_5 (transmission rate from infected fruit bat to susceptible fruit bat) and μ_B (natural death rate for fruit bats). Right: 3D sensitivity of $\mathscr{R}_0^B$ with respect to β_5 and μ_B.

turn, raises the likelihood of disease transmission. This can lead to an increase in $\mathscr{R}_0^B$. Conversely, an increase in the disease transmission rate has a direct and positive relationship with $\mathscr{R}_0^B$. As this rate rises, the probability of transmission from infected bats to susceptible bats becomes greater, contributing to the increase in $\mathscr{R}_0^B$. Therefore, a decrease in the natural mortality rate and an increase in the transmission

rate can significantly influence the potential for disease spread.

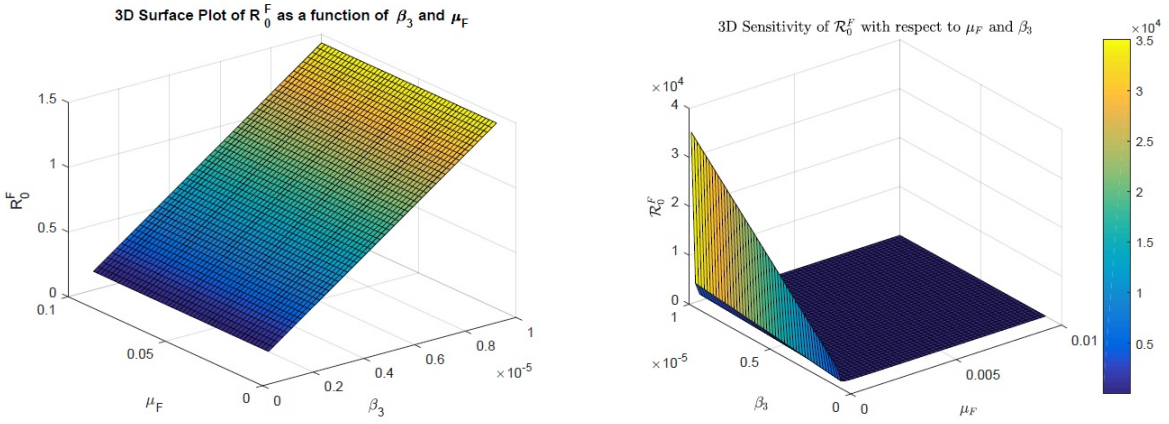

Figure 7: Left: 3D surface plot of $\mathscr{R}_0^F$ as a function of β_3 (transmission rate from infected fruits to susceptible fruits) and μ_F (decay rate of fruits). Right: 3D sensitivity of $\mathscr{R}_0^F$ with respect to β_3 and μ_F.

Figure 7 on the left shows that as β_3 increases while μ_F is kept at a low level, $\mathscr{R}_0^F$ clearly increases. This indicates that the disease transmission rate (β_3) has a greater impact. If β_3 is held constant, an increase in the decay rate of fruits can lead to a decrease in $\mathscr{R}_0^F$, but the effect of β_3 is greater than that.

Figure 7 on the right illustrates the sensitivity of $\mathscr{R}_0^F$ to changes in β_3 and μ_F. The surface of the graph indicates that $\mathscr{R}_0^F$ is highly sensitive to variations in β_3 and μ_F, particularly when the values of β_3 increase. The colors ranging from yellow to blue represent wide variations in the sensitivity of $\mathscr{R}_0^F$. Yellow signifies higher values of $\mathscr{R}_0^F$, while blue indicates lower values. This graph also shows that with an increase in β_3, even at low values of β_3, $\mathscr{R}_0^F$ increases significantly. This highlights the systems high sensitivity to the transmission rate.

In Figure 8, we have displayed the local stability of E^0 point. In this point, the reproduction number $\mathscr{R}_0 = 0.7476$ and $E^0 = (\frac{\Psi_H}{\mu_H}, 0, 0, \frac{\Psi_F}{\mu_F}, 0, \frac{\Psi_B}{\mu_B}, 0) = (135166240, 0, 0, 2239, 0, 3000, 0)$. In this figure, the infective population such as I_H, I_F, and I_B converge to a disease-free equilibrium point (E^0).

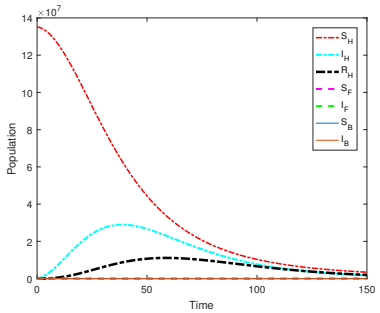

Figure 8: The local stability of E^0 for the model (4)

7 Conclusion

In this article, we investigated a three-layered compartmental model to explain the spread of the Nipah virus, incorporating the role of fruits as intermediate hosts. While prior studies have focused on the role of infected pigs, fewer have considered the intermediate role of fruits, a factor highlighted in our model. Our analysis provides valuable insights into disease dynamics, including equilibrium points and threshold parameters calculated using the next-generation matrix method. Furthermore, we demonstrated the global asymptotic stability of the disease-free equilibrium and used Lyapunov functions for other equilibria. Numerical simulations for Bangladesh (2001-2015) show that our model closely aligns with observed data, supporting the theoretical results. In addition, the sensitivity analysis in our model highlights the importance of parameters like the natural death rate for humans (μ_H), which was not given particular attention in previous models.

Based on the findings of our model, we recommend enhanced surveillance of fruit-fruit bat interactions and human exposure in areas where Nipah outbreaks are prevalent. Further, public health interventions should consider the inclusion of intermediate hosts, such as fruits, in control strategies. Additionally, given the dynamics of the disease, policies for timely recovery and reintegration of previously infected individuals could be crucial in limiting the spread.

Future work could focus on expanding this model to include additional factors, such as environmental conditions, varying immunity durations, and cross-species transmission dynamics. Further exploration of the impact of fruit bat migration patterns and their influence on disease spread would provide a deeper understanding of regional outbreaks. Moreover, extending this model to other regions with similar ecological conditions could offer broader insights into controlling viral epidemics.

Acknowledgments

The authors are grateful to the anonymous reviewers for suggestions which improve the article. All authors approved the final version of the manuscript.

References

[1] R. Amin, Ş. Yüzbaş, S. Nazir, *Efficient Numerical Scheme for the Solution of HIV Infection CD4+ T-Cells Using Haar Wavelet Technique*, CMES Comput. Model. Eng. Sci. **131** (2022) 639–653.

[2] Attaullah, R. Jan, Ş. Yüzbaş, *Dynamical behavior of HIV Infection with the influence of variable source term through Galerkin method*, Chaos Solitons Fractals **152** (2021) 111429.

[3] Attaullah, Ş. Yüzbaş, S. Alyobi, M.F. Yassen, W. Weera, *A Higher-Order Galerkin Time Discretization and Numerical Comparisons for Two Models of HIV Infection*, Comput. Math. Methods Med. **1** (2022) 3599827.

[4] S. Barua, A. Denes, *Global dynamics of a compartmental model for the spread of Nipah virus*, Heliyon **9** (2023) e19682.

[5] S. Barua, M. Ibrahim, A. Denes, *A compartmental model for the spread of Nipah virus in a periodic environment*, AIMS Math. **8** (2023) 29604-29627.

[6] M.H.A. Biswas, M.M. Haque, G. Duvvuru, *A mathematical model for understanding the spread of Nipah fever epidemic in Bangladesh*, International Conference on Industrial Engineering and Operations Management (IEOM) (2015) 1–8.

[7] Y. Chen, J. Li, S. Zou, *Global dynamics of an epidemics model with relapse and nonlinear incidence*, Math. Methods Appl. Sci. **42** (2018)

[8] S. Das, P. Das, P. Das, *Control of Nipah virus outbreak in commercial pig-farm with biosecurity and culling*, Math. Model. Nat. Phenom. **15** (2020) 64.

[9] P.V. Driessche, J. Watmough, *Reproduction numbers and sub-threshold endemic equilibria for compartmental models of disease transmission*, Math Biosci. **180** (2002) 29–48.

[10] J.H. Epstein, S.J. Anthony, A. Islam, et al., *Nipah virus dynamics in bats and implications for spillover to humans*, Proc. Natl. Acad. Sci. **117** (2020) 29190–29201.

[11] N.K. Goswami, F. Hategekimana, *Optimal control techniques for the transmission risk of Nipah virus disease with awareness*, Adv. Syst. Sci. Appl. **4** (2022) 176–192.

[12] R. Jan, M.S. Zobaer, Ş. Yüzbaş, Attaullah, M. Jawad, A. JAN, *Fractional derivative analysis of Asthma with the effect of environmental factors*, Sigma. J. Eng. Nat. Sci. **42** (2024) 177–188.

[13] S. Li, S. Ullah, Samreen, I.U. Khan, S.A. Alqahtani, M.B. Riaz, *A robust computational study for assessing the dynamics and control of emerging zoonotic viral infection with a case study: A novel epidemic modeling approach*, AIP Adv. **14** (2024) 015051.

[14] A.C. Loyinmi, S.O. Gbodogbe, *Mathematical modeling and control strategies for Nipah virus transmission incorporating bat-to-pig-to-human pathway*, EDUCATUM J. Sci. Math. Tech. **11** (2024) 54–80.

[15] M. Parsamanesh, M. Erfanian *Global dynamics of an epidemic model with standard incidence rate and vaccination strategy*, Chaos Solitons Fractals **117** (2018) 192–199.

[16] M. Parsamanesh, M. Erfanian, S. Mehrshad, *Stability and bifurcations in a discrete-time epidemic model with vaccination and vital dynamics*, BMC Bioinformatics **21** (2020) 525.

[17] M. Parsamanesh, M. Erfanian, *Stability and bifurcations in a discrete-time SIVS model with saturated incidence rate*, Chaos Solitons Fractals **150** (2021) 111178.

[18] Samreen, S. Ullah, R. Nawaz, S.A. Alqahtani, S. Li, A. Hassan, *A mathematical study unfolding the transmission and control of deadly Nipah virus infection under optimized preventive measures: New insights using fractional calculus*, Results in Phys. **51** (2023) 106629.

[19] N.H. Shah, N. Trivedi, F. Thakkar, M. Satia, *Control strategies for Nipah virus*, Int. J. Appl. Eng. Res. **13** (2018) 21.

[20] H. Smith, *An Introduction to Delay Differential Equation with Applications to the Life Sciences*, Springer, New York, 2011.

[21] G. Yildirim, Ş. Yüzbaş, A Collocation Technique via Pell-Lucas Polynomials to Solve Fractional Differential Equation Model for HIV/AIDS with Treatment Compartment, Comput. Model. Eng. Sci. **141** (2024).

[22] G. Yildirim, Ş. Yüzbaş, *Numerical solutions and simulations of the fractional COVID-19 model via PellLucas collocation algorithm*, Math. Methods. Appl. Sci. **47** (2024) 14457–14475.

[23] G. Yildirim, Ş. Yüzbaş, *Numerical solutions of SIRD model of Covid-19 by utilizing Pell- Lucas collocation methodLucascollocation method*, Turk. J. Math. **48** (2024) 1156–1182.

[24] Ş. Yüzbaş, *A numerical approach to solve the model for HIV infection of CD4 + T cells*, Appl. Math. Model. **36** (2012) 5876–5890.